

Classifying Time-Varying Complex Networks on the Tensor Manifold

Romeil Sandhu

romeil.sandhu@stonybrook.edu

Departments of Biomedical Informatics, Computer Science and Applied Mathematics/Statistics

Stony Brook University, Stony Brook, NY 11794

Abstract

At the core of understanding dynamical systems is the ability to maintain and control the systems behavior that includes notions of robustness, heterogeneity, and/or regime-shift detection. Recently, to explore such functional properties, a convenient representation has been to model such dynamical systems as a weighted graph consisting of a finite, but very large number of interacting agents. This said, there exists very limited relevant statistical theory that is able cope with real-life data, i.e., how does perform simple analysis and/or statistics over a “family” of networks as opposed to a specific network or network-to-network variation. Here, we are interested in the analysis of network families whereby each network represents a “point” on an underlying statistical manifold. From this, we explore the Riemannian structure of the statistical (tensor) manifold in order to define notions of “geodesics” or shortest distance amongst such points as well as a statistical framework for time-varying complex networks for which we can utilize in higher order classification tasks.

1. Introduction

Notions of robustness, heterogeneity, and phase changes are ubiquitous concepts employed in understanding complex dynamical systems with a variety of applications [1, 2, 3, 4]. This is seen in Figure 1. While recent advancements in network analysis has arisen through the usage of spectral techniques [5], expander graphs [6], percolation theory [7], information theoretic approaches [8, 9], scale-free networks [4], and a myriad of graph measures reliant on the underlying discrete graph space (e.g., degree distribution [10], shortest path [8], centrality [11, 12, 13]), such measures rarely incorporate the underlying dynamics in its construction. Limitations of such static measures can be more aptly seen in multilayer networks whereby standard network measures are immediately ambiguous; shortest paths

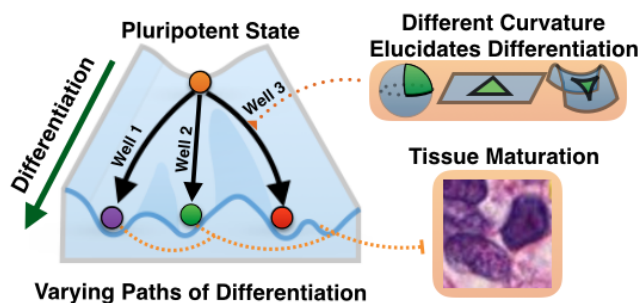


Figure 1. This work focuses on the exploiting the underlying geometry in a statistical framework to elucidate regime-shifts and bifurcation detection in dynamical systems. We apply our analysis towards broader cell differentiation and signaling promiscuity in biological systems with cancer applications (e.g., inducing terminal homogeneous state from a pluripotent stem-cell like state)

(geodesics) are non-trivial [14] while centrality measures [15], clustering methods [16], and diffusion models [17] require simplifications to make sense of real-world configurations. Moreover, static properties have been unable to model time-varying nonlinear higher order effects (e.g., targeted therapy [18], cellular reprogramming [19]) which can be seen pictorially in Figure 1 and Figure 2. This is akin to waterbed theory which refers to the observation of when a complex behavior is “pushed” down, the invariable effect of complexity causes for that behavior to “pop-up” elsewhere [20].

To this end, we have previously developed fundamental relationships between network functionality [8, 21] and certain topological and geometric properties of the corresponding graph [22, 23]. In particular, recent work of ours has shown the geometric notion of curvature (a measure of “flatness”) is positively correlated with a system’s robustness or its ability to adapt to dynamic changes [24, 25]. This can be seen in Figure 3A. In this regard, network curvature may relate to anomaly detection [26], congestion in communication [27, 28], drug resistance [29], supply chain risk [30], to

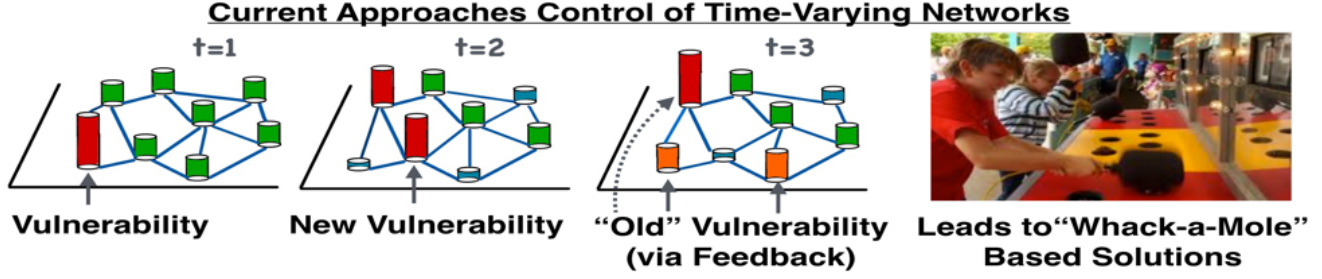


Figure 2. Current modeling of static network properties leads to ill-posed “whack-a-mole”-based solutions whereby to alter functionality, one “whacks” a vulnerabilities of a system at a given time t . However, due to heterogeneity, this leads to new vulnerabilities and further (perhaps accelerated) breakdown via feedback.

even systemic risk in banking systems [31, 32]. Moreover, this is particularly compelling since curvature can be readily computed for large-scale networks using theory from optimal mass transport [33], and more importantly, highlights the significance of employing geometry in network analysis. This said, there exists very limited relevant statistical theory that is able cope with a *family of networks* and one often focuses on a given network or is limited to measures that exploit network-to-network variations as it pertains to functionality. *Here, we are interested in expounding upon previous work [24] in order to exploit statistics over a family of networks such that higher order classification tasks can be performed to better understand regime shifts.*

To do so, we are interested in studying geometry of networks as a dynamical system that evolves over time in which each given network or observation may represent a “point” (encoded by *some* matrix-based positive definite model) on an underlying Riemannian manifold. From this, we are interested in defining geodesics such that distances between “points” (networks) in a given a family can be measured and proper statistical analysis can be achieved. For a broad range of problems, such information may include, but not limited to, vector-valued time series, power spectral density [34], to density matrices from quantum mechanics that aptly describes the mixed state of the system [35]. In general, the set of Hermitian positive definite (PD) matrices plays a fundamental role in a variety of engineering applications with the most recent attention renewed on developing lower order statistics [36, 37, 38, 39]. In relationship to this mathematical structure, significant related work on employing statistical analysis for Riemannian manifolds has focused on directional statistics, statistics on shape spaces, as well as specific manifolds - we refer the reader [40, 41, 42] and references therein. This being said, while these methods are mostly extrinsic whereby one embeds the manifold in an ambient Euclidean space, we are interested in studying *intrinsic* Riemannian metrics that can be naturally applied to the network setting without restrictions on the network topology. For example, from a network geometric per-

spective, there has been very interesting work modeling the space of tree-like structures in understanding phylogenetic trees for cancer and evolutionary biology [43, 44]. Recently, phylogenetic trees were shown to live in a negatively curved space [43] resulting in a new push to develop an appropriate statistical framework (i.e., if a manifold is negatively curved, then one can define a unique geodesic). This has led to methods in hierarchical learning and clustering [45]. Nevertheless, as seen in Figure 4, non tree-like networks still “live” upon some Riemannian (statistical) manifold for which we need to construct a framework capable of resolving unique geodesics (shortest path) amongst such points. In turn, we can then perform statistics on this space allowing us to classify certain behaviors and operating regimes which will be key to maintaining control and avoiding shotgun-based solutions during “black swan” events [46] whereby the continuous failing of interacting agents may result in catastrophic failure.

The remainder of the present paper is outlined as follows: In the next section, we first provide important preliminaries in motivating the theoretical need of understanding geometry by revisiting curvature and entropy as it pertains to functionality. Here, we see that *changes* in the geometry provides intrinsic information about the dynamic system and thus, its exploration fits towards a larger program developed in this paper and current related work [24, 25]. From this, Section 3 lays the foundation of a Riemannian framework previously employed for Diffusion Tensor Imaging whereby we now adapt such notions towards complex networks. Then, Section 4 presents preliminary results on synthetic and biological data. We conclude with a summary and future work in Section 5.

2. Geometry and System Behavior

To illustrate how geometry elucidates the functional behavior of a dynamical system and how such ingredients are ever-important the analysis and control of time-varying networks, let us revisit optimal mass transport (OMT) [33].

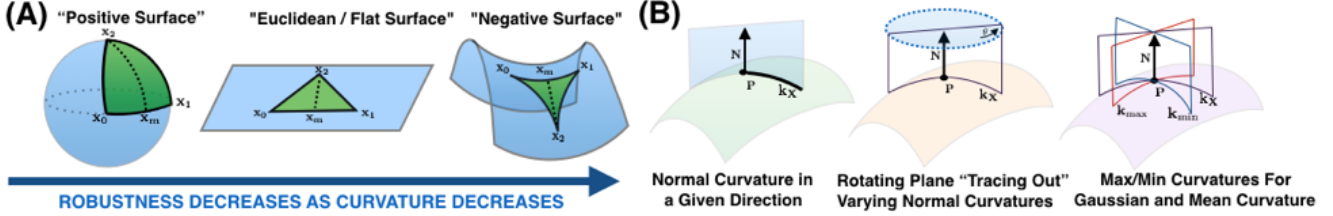


Figure 3. Visual illustration of curvature. (A) The thematic and motivating vision of this work is based on the above-illustrated result [24, 25]. (B) Other forms of curvature that play important roles in (projective) geometry and machine learning.

The first notion of OMT was proposed by Gaspar Monge in 1781 with the concern of finding the minimal transportation cost for moving a pile of soil from one site to another. The modern formulation, given by Kantorovich, has been ubiquitously used in fields of econometrics, fluid dynamics, to shape analysis [33, 47, 48] and recently, has received a renewed mathematical interest [49, 50]. More formally, let (X, μ_0) and (Y, μ_1) be two probability spaces and let $\pi(\mu_0, \mu_1)$ denote the set of all couplings on $X \times Y$ whose marginals are μ_0 and μ_1 . As such, the Kantorovich costs seeks to minimize $\int c(x, y) d\pi(x, y) \forall \pi \in \pi(\mu_0, \mu_1)$ where $c(x, y)$ is the cost for transporting one unit of mass from x to y . The cost originally defined in a distance form on a metric space leads to the L^p Wasserstein distance as follows:

$$W_p(\mu_1, \mu_2) := \left(\inf_{\mu \in \pi(\mu_0, \mu_1)} \int \int d(x, y)^p d\mu(x, y) \right)^{\frac{1}{p}} \quad (1)$$

From this, let us begin considering M to be a Riemannian manifold for which “points” are now defined

$$\begin{aligned} \mathcal{P} &:= \{ \mu \geq 0 : \int \mu \, d\text{vol}(M) = 1 \} \\ \mathcal{T}_\mu \mathcal{P} &:= \{ \eta : \int \eta \, d\text{vol}(M) = 0 \} \end{aligned} \quad (2)$$

as the space of probability densities and the tangent space at a given point μ , respectively. Due to the work of Benamou and Brenier [48], one can naturally compute the geodesic (in the Wasserstein sense) between two densities $\mu_0, \mu_1 \in \mathcal{P}$ as the below **optimal control problem**:

$$\begin{aligned} \inf_{\mu, g} & \left\{ \int \int_0^1 \mu(t, x) \|\nabla g(t, x)\| dt d\text{vol}(M) \right. \\ & \text{subject to } \frac{\partial \mu}{\partial t} + \text{div}(\mu \nabla g) = 0 \\ & \left. \mu(0, \cdot) = \mu_0, \quad \mu(1, \cdot) = \mu_1 \right\} \end{aligned} \quad (3)$$

which leads us to give \mathcal{P} a Riemannian structure due to some very nice work of Jordan *et. al* [51]. Armed with this, we are now able to see how changes to the underlying geometry (namely curvature) may serve as a proxy for

system behavior (namely functional robustness). As such, let

$$H(\mu_t) := \int_M \log \mu_t d\text{vol}(M) \quad (4)$$

represent Boltzmann entropy where the dependency on x has been dropped for convenience and we consider a family of densities evolving over time. Taking the second variation with respect to time t in the Wasserstein sense (i.e., our gradient steps are taken to minimize or maximize the Wasserstein distance rather than the classical Euclidean norm) and noting that, by construction, $\eta := \frac{\partial \mu}{\partial t}|_{t=0}$, we have that

$$\begin{aligned} \frac{d^2}{dt^2} H(\mu_t)|_{t=0} &= \langle \text{Hess}(H)(\eta), \eta \rangle_W \\ &= - \int_M \langle \nabla g_\eta, \nabla \Delta g_\eta \rangle + \frac{1}{2} \Delta(\|\nabla g_\eta\|^2) \mu_0 d\text{vol}(M) \end{aligned} \quad (5)$$

where μ_0 and g_η satisfy equation (3). Using the Bochner formula [54], which relates harmonic functions on a Riemannian manifold to Ricci curvature (a geometric measure of “flatness” and herein denoted as “Ric”), we can further assume $\text{Ric} \geq kI$ as quadratic forms where k is a constant and I is the identity matrix. Then, **due to a beautiful result of Sturm [53] as well as Lott and Villani [33]**, one can show that the $\text{Hess}(H)$ is k -convex with respect to the Wasserstein norm:

$$H(\mu_t) \leq tH(\mu_0) + (1-t)H(\mu_1) - \phi(k, t, \mu_0, \mu_1) \forall t \in [0, 1] \quad (6)$$

where the right hand portion of the above equation denoted as $\phi(\cdot)$ can be shown to be $\phi(k, t, \mu_0, \mu_1) = \frac{k}{2} t(1-t) W_2(\mu_0, \mu_1)^2$ allowing for k -convexity. That is, changes in entropy and curvature are positively correlated, i.e., $\Delta H \times \Delta \text{Ric} \geq 0$. Now, let $p_\epsilon(t)$ denote that probability that the mean of a given observable deviates by more than ϵ from the original (unperturbed) value at time t . Then from large deviations theory, one can define a rate function as:

$$R := \lim_{t \rightarrow \infty, \epsilon \rightarrow 0} \left(-\frac{1}{t} \log p_\epsilon(t) \right) \quad (7)$$

Therefore, a large R means a fast return to the original state (robustness), and a small R corresponds to a slow return

(fragility). In thermodynamics, it is well-known that entropy and rate functions from large deviations are closely related [21]; the Fluctuation Theorem [8] is an expression of this fact for complex networks and may be expressed as $\Delta H \times \Delta R \geq 0$. With the result of equation (6), we have

$$\Delta Ric \times \Delta R \geq 0 \quad (8)$$

which states that changes in Ricci curvature are positively correlated to changes in robustness. Perhaps more importantly, **the manner in which the underlying geometry changes elucidates certain behaviors of a complex dynamical system** and this stylized fact, sets the motivation for this note in which we attempt to generalize statistics to a family of networks that live on a certain manifold.

2.1. Scalar Model: Network-to-Network Analysis

As highlighted in the previous section, geometry of networks plays an integral role in understanding functionality. In particular, in the scalar case with the structure given by equation (2), one can discretely defined Ricci Curvature (due to Ollivier [22]) between any two “points” x and y as:

$$\kappa(x, y) := 1 - \frac{W_1(\mu_x, \mu_y)}{d(x, y)} \quad (9)$$

This definition, motivated by coarse geometry, is applicable to the graph setting whereby the geodesic distance $d(x, y)$ is given by the hop metric and W_1 can be computed simply via linear programming [55]. However, this measure is limited to local network-to-network variation as opposed to a family of networks and as such, we require a generalization to the matrix valued setting; a non-trivial problem that has been recently studied [50]. Therefore, this note and latter (future) work will seek to construct matrix-valued curvature based measures. To do so, we first need notion of matrix-valued distance $d_M(x, y)$.

3. Manifold of Time-Varying Networks

This section will introduce a framework capable of defining statistics on a family of networks as seen in Figure 4.

3.1. Geodesics on the Network Manifold

Consider a dynamical system that evolves over time and whose information is encapsulated by a positive definite matrix (tensor). In this regard, it is well-known that the space of tensors is not a vector space, but instead forms a Riemannian manifold M [56]. In particular, we will leverage the theory of symmetric spaces which has been extensively studied since the seminal work of Nomizu [57]; a comprehensive work on tensor manifolds can be found in [58, 59]. Riemannian manifolds are endowed with a metric that smoothly assign to each point $\rho \in M$ an inner product

on \mathcal{T}_ρ , the tangent space to M at ρ . More formally, let us denote Υ and Υ^+ and as the set of all Hermitian matrices and the cone of positive-definite matrices, respectively. We may then define an analogous structure to equation (2) as:

$$\begin{aligned} \Lambda_+ &:= \{\rho \in \Upsilon^+ \mid \text{tr}(\rho) = 1\} \\ \mathcal{T}_\rho &:= \{\chi \in \Upsilon \mid \text{tr}(\chi) = 0\} \end{aligned} \quad (10)$$

where Λ_+ represents our space of networks and \mathcal{T}_ρ is the corresponding tangent space. From this, we let the observations of our dynamic system be recorded as $\{\rho_0, \rho_1, \rho_2, \dots, \rho_t\}$ and where each “point” (network) $\rho_i \in \Upsilon^+$ is given by a tensor. As seen in Figure 4, we need a sensible notion of distance that is dependent on the underlying geometry to define statistics for classification. To do, one defines the *exponential map* as the function that maps to each vector $\overline{\rho_0 \rho_1} \in \mathcal{T}_{\rho_0}$, the point $\rho_1 \in \Lambda_+$ on the manifold M that is reached after unit time by the geodesic starting at ρ_0 with this tangent vector. The exponential map, herein denoted as $\exp_\rho : \mathcal{T}_\rho \mapsto M$ at point ρ is defined on the whole tangent space and for the particular space of tensors, this map is also one-to-one. Moreover, one can also define a unique inverse map denoted as the *logarithm map* $\text{Log}_{\rho_0} : M \mapsto \mathcal{T}_{\rho_0}$ that maps a point $\rho_1 \in M$ to the unique tangent vector $\chi \in \mathcal{T}_{\rho_0}$ at ρ_0 whose initial velocity is that of the unique geodesic γ with $\gamma(0) = \rho_0$ and $\gamma(1) = \rho_1$.

Thus, the problem of classifying time-varying networks amounts to being able to properly computing geodesics on this space and for which, we must now consider a family of curves $\gamma(t)$ on the manifold and its speed vector $\dot{\gamma}(t)$. Then, in the general setting, our geodesic will be a curve that realizes the minimum distance (length) between any two points, e.g., ρ_0 and ρ_1 . That is, we want to compute:

$$\begin{aligned} \mathcal{L}_{\rho_0}^{\rho_1} &= \min_{\gamma} \int_{\rho_0}^{\rho_1} \|\dot{\gamma}(t)\|_{\gamma(t)} dt \\ &= \min_{\gamma} \int_{\rho_0}^{\rho_1} \left(\langle \dot{\gamma}(t), \dot{\gamma}(t) \rangle_{\gamma(t)} \right) \end{aligned} \quad (11)$$

where $\gamma(0) = \rho_0$ and $\gamma(1) = \rho_1$. Given this, we seek to exploit the Riemannian structure of the tensor space proposed by Pennec [59] towards the network setting; most recently used in Diffusion Tensor Imaging [60, 61]. Here, authors utilize a result from differential geometry regarding geodesics for invariant metrics on affine symmetric spaces [62, 63] together with the Sylvester equation from control, to propose an affine invariant metric whereby the unique geodesic curve from point ρ (and at the origin) on our network manifold with a tangent vector χ can be shown to be

$$\begin{aligned} \gamma(t)_{(\rho, \chi)} &= \rho^{\frac{1}{2}} \exp(t\rho^{-\frac{1}{2}} \chi \rho^{-\frac{1}{2}}) \rho^{\frac{1}{2}} \\ \gamma(t)_{(I, \chi)} &= \exp(t\chi) \end{aligned} \quad (12)$$

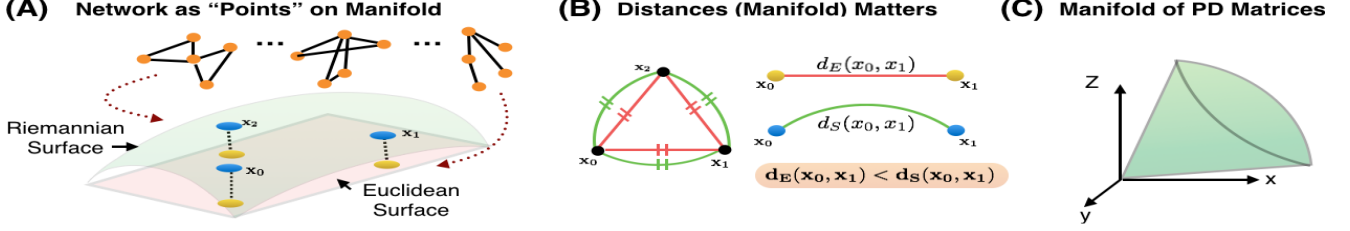


Figure 4. (A) To understand more global functionality, we treat time-varying networks as “points” on a manifold. (B) The study geodesics is needed in order to compute a statistical framework for a family of networks. (C) Manifold of Positive Definite Matrices

where $\exp(\chi) = \sum_{k=0}^{+\infty} \frac{\chi^k}{k!}$ is the usual matrix exponential. From this, the speed vector $\dot{\gamma}(t)$ can be computed:

$$\begin{aligned} \frac{d\gamma(t)}{dt} &= \frac{d}{dt} \exp(t\chi) \\ &= \frac{d}{dt} \left(Q \begin{bmatrix} e^{t\chi_{1,1}} & 0 & \dots & 0 \\ 0 & e^{t\chi_{2,2}} & \dots & 0 \\ 0 & 0 & \dots & e^{t\chi_{n,n}} \end{bmatrix} Q^T \right) \\ &= Q \text{DIAG}(\chi_i \exp(t\chi_i)) Q^T \\ &= \exp(t\chi)^{\frac{1}{2}} \chi \exp(t\chi)^{\frac{1}{2}} \\ &= \gamma(t)^{\frac{1}{2}}_{(I,\chi)} \star \chi \end{aligned} \quad (13)$$

where the $A \star B = ABA^T$. Noting the geodesic $\gamma(t)_{(\rho,\chi)}$ between any two points $\rho_0, \rho_1 \in M$ where $\rho_1 = \exp_{\rho_0}(\chi)$ at $t = 1$, the *logarithm map* can be seen as

$$\begin{aligned} \gamma(1)_{(\rho_0,\chi)} &= \rho_1 = \rho_0^{\frac{1}{2}} \exp(\rho_0^{-\frac{1}{2}} \chi \rho_0^{-\frac{1}{2}}) \rho_0^{\frac{1}{2}} \\ \log(\rho_0^{-\frac{1}{2}} \rho_1 \rho_0^{-\frac{1}{2}}) &= \rho_0^{-\frac{1}{2}} \chi \rho_0^{-\frac{1}{2}} \\ \rho_0^{\frac{1}{2}} \log(\rho_0^{-\frac{1}{2}} \rho_1 \rho_0^{-\frac{1}{2}}) \rho_0^{\frac{1}{2}} &= \chi = \overrightarrow{\rho_0 \rho_1} = \text{Log}_{\rho_0}(\rho_1) \end{aligned} \quad (14)$$

From this, the distance between networks can finally be computed as

$$\begin{aligned} \text{dist}^2(\rho_0, \rho_1) &= \|\text{Log}_{\rho_0}(\rho_1)\|_{\rho_0}^2 \\ &= \|\log(\rho_0^{-\frac{1}{2}} \rho_1 \rho_0^{-\frac{1}{2}})\|_2^2. \end{aligned} \quad (15)$$

We now have a natural distance that measures the length of the geodesic curve that connects any two “points” on our network manifold. This is particularly important as we can now begin to perform statistics over a family of networks.

3.2. Mean, Variance, Mahalanobis Distance

Given the above geodesic distance, one can formulate necessary statistics on our network manifold. Using the framework established by Pennec [59] with the above affine invariant metric, the unique mean $\bar{\rho}$ of N “points” $\{\rho_0, \rho_1, \rho_2, \dots, \rho_N\}$ on the tensor manifold can be computed via gradient descent:

$$\bar{\rho}_{t+1} = \bar{\rho}_t^{\frac{1}{2}} \exp \left(\frac{1}{N} \sum_{i=1}^N \log \left(\bar{\rho}_t^{-\frac{1}{2}} \rho_i \bar{\rho}_t^{-\frac{1}{2}} \right) \right) \bar{\rho}_t^{\frac{1}{2}} \quad (16)$$

It has been noted that although no closed form expression for the mean exists, the above converges towards a steady-state solution in a few iterations. As in the traditional Euclidean distance and similar to the Karcher or Frechet mean, the above mean is constructed on the premise that we seek a “point” that minimizes the sum of squared distance, i.e., $\rho = \sum_{i=1}^N \text{dist}^2(\rho, \rho_i)$. In a similar fashion, the variance can be computed as follows:

$$\Sigma = \frac{1}{N-1} \sum_{i=1}^N \text{Vec}_{\bar{\rho}}(\text{Log}_{\bar{\rho}}(\rho_i)) \text{Vec}_{\bar{\rho}}(\text{Log}_{\bar{\rho}}(\rho_i))^T \quad (17)$$

where $\text{Vec}_{\bar{\rho}}(\rho_i) = \text{Vec}_I(\log(\bar{\rho} \star \rho_i))$ and where the operation $\text{Vec}_I(A)$ is a vectorized projection of the independent coefficients of our tensor in the above formulation, i.e., $\text{Vec}_I(A) = (a_{1,1}, \sqrt{2}a_{1,2}, \dots, \sqrt{2}a_{1,n}, \dots, \sqrt{2}a_{n-1,n}, a_{n,n})$. From this, one obtains a generalized form of the Gaussian distribution on the tensor manifold as:

$$N_{(\bar{\rho}, \Sigma)}(\rho_i) = k \exp \left(-\frac{1}{2} \xi_{(\bar{\rho}, \Sigma)}(\rho_i) \right) \quad (18)$$

where $\xi_{(\bar{\rho}, \Sigma)}$ represents the classic Mahalanobis distance now defined in the Riemannian setting as seen below

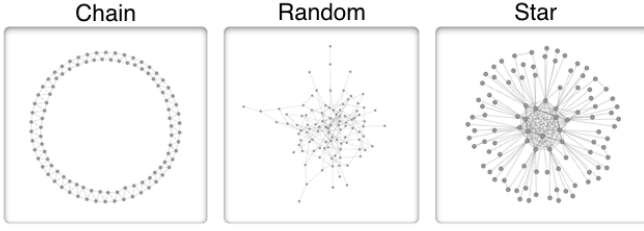
$$\xi_{(\bar{\rho}, \Sigma)}(\rho_i) = \text{Vec}_{\bar{\rho}}(\text{Log}_{\bar{\rho}}(\rho_i))^T \Sigma \text{Vec}_{\bar{\rho}}(\text{Log}_{\bar{\rho}}(\rho_i)). \quad (19)$$

While the above provides a few basic tools, we have omitted, for the sake of brevity varying other advantages that can be employed towards the network setting through the framework established above. This will be a subject of future work in which powerful tools, previously employed for DTI imaging, will now be used to exploit time-varying networks. Of course, to do so, we need to define our matrix-based model that will allow for networks to be represented on the tensor manifold. This is discussed next.

3.3. Matrix-Based Model: Graph Laplacian

Given that we are focused network control, we employ an approximated graph Laplacian as our matrix-based model whose structure provides a global representation of a given network with many useful properties that are intrinsically tied to system functionality. While a complete review

(A) Synthetic Toy (“Communication”) Configurations



(B) Network Distance Under Varying Uniform Noise

RIEMANNIAN DISTANCE	[1,1]	[.75,1]	[.5,1]	[.25,1]	[0,1]
CHAIN v.s. STAR	14.23	14.23	14.30	14.50	15.25
CHAIN v.s. RANDOM	14.85	14.88	14.98	15.29	16.13
STAR v.s. RANDOM	11.55	11.57	11.57	11.78	12.25
EUCLIDEAN DISTANCE	[1,1]	[.75,1]	[.5,1]	[.25,1]	[0,1]
CHAIN v.s. STAR	5.88	5.87	5.90	6.01	6.30
CHAIN v.s. RANDOM	6.99	7.00	7.08	7.18	7.63
STAR v.s. RANDOM	6.09	6.10	6.10	6.24	6.48

Figure 5. (A) Graphical view of the three synthetic “toy” graphs that can be representative of varying types of communication networks, each with 200 nodes and 400 edges (i.e., only topology changes). (B) Distances of network-to-network under varying weights or “noise.” We see that the proposed framework is able to properly quantify difference as compared to Euclidean measure, i.e., the star-like network is “closest” to the random network as supported in [8, 24].

is beyond the scope of this note (we refer the reader to [5]), a few areas that have garnered attention have included construction of expander graphs [6] to Cheegers inequality with increasing attention on connections between spectral graph theory and its respective geometry [64]. Mathematically, one can define the Laplacian operator for a specific network as $\Delta f(x) = f(x) - \sum_y f(y) \mu_x(y)$ with f being a real-valued function which coincides with the usual normalized graph Laplacian given by:

$$L = I - D^{-\frac{1}{2}} A D^{-\frac{1}{2}} \quad (20)$$

It is interesting to note in this connection that if $k \leq \kappa(x, y)$ is a lower bound for Ricci curvature defined in equation (9), then the eigenvalues of Laplacian is bounded $k \leq \lambda_2 \leq \dots \leq \lambda_N \leq 2 - k$ [64]. This relationship is important since $2 - \lambda_N$ measures the deviation of the graph from being bipartite, i.e., a graph whose vertices can be divided into two disjoint sets U and V such that every edge connects a vertex in U to one in V . As such ideas appear in resource allocation and control, the study of such structures in the time-varying setting motivate our focus on the Laplacian matrix. Lastly, while one can form a normalized Laplacian with unitary trace, we note that the Laplacian matrix by definition is a positive semi-definite matrix. Therefore, to enforce positive definiteness, we utilized an approximated Laplacian $\hat{L} := L + \epsilon_L I$ where $0 < \epsilon_L \ll 1$ such that $x^T \hat{L} x > 0$ for all nonzero $x \in \mathbb{R}^n$.

4. Results

We now present preliminary results. While these experiments are by no means exhaustive (and will be extended), these results highlight potential of the above framework for time-varying network analysis.

4.1. Toy Network Configurations

To provide initial intuition of the proposed framework, we constructed three toy “communication” based networks.

As one can see in Figure 5, the networks are composed of 200 nodes and 400 edges with varying topology that represents a chain, a random, and a star-like network. Similar to our earlier work [24], we are interested in using the proposed framework to measure distances amongst these structures under varying “noise”. As highlighted by network curvature [24] and network entropy [8], one should expect from a communication perspective the star-like network is “closer” to a “random” network. That is, given that their functional properties such as robustness (a measure of “flatness”) are similar compared towards the chain-like network, we should expect that such networks on the manifold lie closer to one another. This is exactly what is shown in Figure 5B. Moreover, as we move from an unweighted graph to a weighted graph in which weights are chosen randomly in a uniform manner, this relationship still holds. On the other hand, if we utilize the classical Euclidean distance (Frobenius norm) to measure network-to-network distance, we find that the chain-like network is in fact “closer” to the star-like network. From a communications perspective, this does not make sense and highlights the proposed framework. Lastly, it is interestingly to see that as we increase the support of weight selection, the distances between such networks increases as to be expected.

4.2. Scale-Free and Random Networks

This section presents clustering results and the importance of exploiting the underlying geometry as it relates scale-free networks. In particular, we generate 50 scale-free networks (i.e., degree distribution follows power law) [1] and 50 random (Erdos-Renyi) networks with each network composed 200 nodes and 1164 edges (differences are only in topology). Such scale-free networks stylistically could represent “business as usual” behavior while such random networks may represent a particular crisis in which structure (correlation of agents) breaks down. From this, one can generate an approximated normalized graph Laplacian

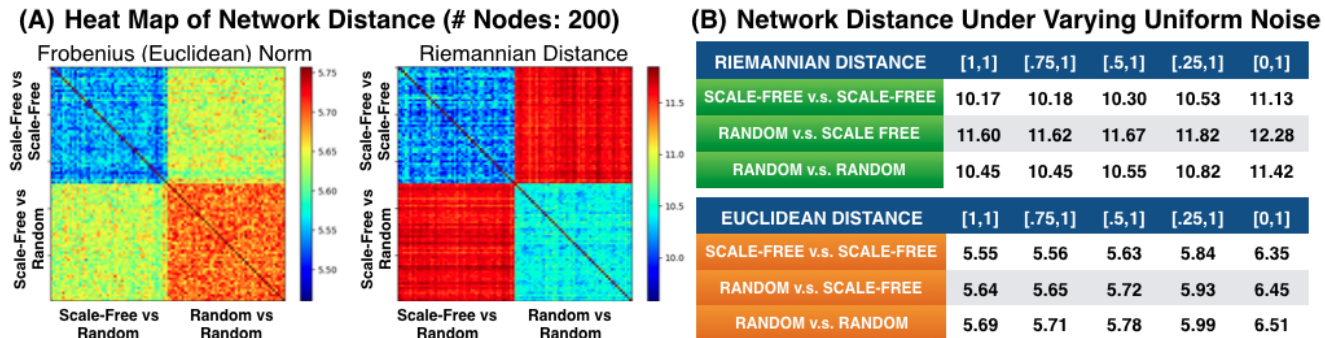


Figure 6. Heat map of distances between scale-free and random networks measured by the proposed Riemannian metric to that of the Frobenius norm. (B) Average distance of network-to-network under varying weights or “noise.” We see that the proposed framework is able to properly quantify difference as compared to Euclidean measure. Note: Each random and scale-free network possess same number of nodes and edges, only topology changed.

as defined in Section 3.3 whereby each network now represents a point on our tensor manifold. In doing so, we compute pairwise distances amongst all potential network pairs based on the Euclidean distance, defined by the Frobenius norm, as well as the Riemannian distance, defined by equation (15). Figure 6A presents a “heat map” of the distances. As one can see, Euclidean distance fails to cluster networks as the distance between scale-free to random networks are “closer” than random to random networks. The framework proposed here is able to properly cluster the aforementioned networks highlighting the thematic importance of using Riemannian geometry when exploiting distances and/or similarity measures. Figure 6B also presents average distances amongst scale-free-to-scale-free, random-to-scale-free, and random-to-random networks. Lastly, we note that if the above experiments were repeated and/or the number of nodes/edges were changed, the clustering result would still hold.

4.3. Waddingtons Landscape: Cell Differentiation

In this section, we now turn our attention in utilizing the proposed framework towards a regime shifts of cellular differentiation of Waddington’s Landscape as depicted in Figure 1. This epigenetic landscape provides a stylistic hierarchical view cellular differentiation [65], i.e., landscape elevation associates to varying degrees of pluripotency or the ability for a cell to differentiate to multiple function specific tissues. That is, pluripotent and progenitor cells are “higher” compared to a further differentiated state whether that be another function specific stem-cell or tissue. Nevertheless, at a high level, one can consider the intricate and complex processes of cellular differentiation as a interconnected dynamical system (network) whereby such bifurcations or regime-shift relate to differentiated states that lie on Waddington’s landscape [66].

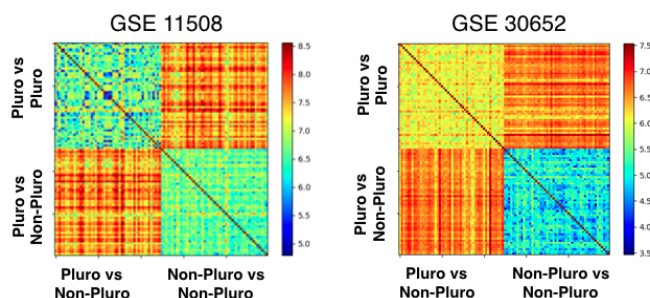
To illustrate this and from a classification perspective, we

accessed the Gene Expression Omnibus (GEO). In particular, we selected two public datasets, GSE11508 and GSE 30652, that possess 59 pluripotent / 160 non-pluripotent and 159 pluripotent / 32 non-pluripotent cell samples, respectively. Within each pluripotent samples of both datasets, there contains varying types that include human embryonic stem cells (hESCs) and induced pluripotent stem cells (iPSCs). This results in a potential mix of differentiation, i.e., iPSCs pluripotency may be much lower than hESCs yet are deemed pluripotent. Here, we are primarily interested to examine how “far” apart differentiated samples are from their counterparts and would be key in devising a necessary quantitative framework characterizing Waddingtons Landscape. As such, through the use of the KEGG database downloaded from Pathway Commons, we construct a single pluripotent network whereby the weights are the gene-to-gene correlation of twenty random pluripotent samples selected from each of the respective data sets. This was done similarly for a single non-pluripotent network. Together, this was repeated to generate 50 pluripotent and non-pluripotent networks from each GSE11508 and GSE 30652. Figure 7 presents heat map results as well as the average network distance between such networks. As one can see, we see a marked increase in distance between pluro and non-pluro samples. We note the Frobenius norm follows this same pattern and can primarily be attributed to the fact that we fixed the topology between pluro/non-pluro networks, the small number of samples for correlation, as well as the dependency of our underlying interactome KEGG network. This said, we have presented such results here to motivate the need for future work.

5. Summary & Conclusion

This note introduces a statistical geometric framework [59] towards time-varying network analysis. While such

(A) Heat Map of Cellular Differentiation



(B) Network Distance of Pluripotency

GSE: 11508	PLURO v.s. PLURO	PLURO v.s. NON-PLURO	NON-PLURO v.s. NON-PLURO
RIEMANNIAN DISTANCE	6.55	7.55	6.60
EUCLIDEAN DISTANCE	1.24	1.72	1.35

GSE: 30652	PLURO v.s. PLURO	PLURO v.s. NON-PLURO	NON-PLURO v.s. NON-PLURO
RIEMANNIAN DISTANCE	6.11	6.61	4.99
EUCLIDEAN DISTANCE	1.45	1.67	0.94

Figure 7. Heat map of Riemannian distances between pluripotent and non-pluripotent networks under two public datasets. (B) Average numerical distance between the pluro and non-pluro networks. We see the proposed measure is able to classify such samples as well as the Euclidean measure. We note the topology here is fixed across each networks unlike previous synthetic results.

mathematical concepts have been successfully employed for DTI Imaging [61], the underlying structure is equally relevant in the classification of regime-shifts in networks. To illustrate the importance of geometry in this setting, we presented preliminary results that show classical Euclidean distances are unable to properly differentiate between not only toy network configurations, but that of scale-free and random networks. We concluded with an example of how the proposed framework may be utilized on real-life biological stem-cell data. Putting this all together, these preliminary results and methodology set the foundation for a more expansive study on global notions of robustness, heterogeneity, and/or regime-shift detection.

References

- [1] A. Barabasi. "The Network Takeover," *Nature Physics*. 2012. 1, 6
- [2] H. Kitano. "Cancer as a robust system: implications for anticancer therapy." *Nature Reviews Cancer*. 2004. 1
- [3] M. Csete and J. Doyle. "Reverse engineering of biological complexity." *Science*. 2002. 1
- [4] A. Barabasi and R. Albert. "Emergence of Scaling Random Networks." *Science*. 1999. 1
- [5] R.K. Fan Chung. "Spectral Graph Theory." *American Mathematical Society*. 1997. 1, 6
- [6] S. Hoory, N. Linial, and A. Wigderson. "Expander Graphs and Their Applications." *American Mathematical Society*. 2006. 1, 6
- [7] D. Stauffer and A. Aharony. "Introduction to Percolation Theory." *Taylor and Francis*. 1994 1
- [8] L. Demetrius and T. Manke. "Robustness and Network Evolution: Entropic principle." *Physica A: Statistical Mechanics and its Applications*. 2005. 1, 4, 6
- [9] J. West, G. Bianconi, S. Severini, and A. Teschen-dorff. "Differential Network Entropy Reveals Cancer System Hallmarks." *Nature (Scientific reports)* 2012. 1
- [10] I. Taylor, R. Lindling, D. Warde-Farley, Y. Liu, C. Pesquita, D. Faria, S. Bull, T. Pawson, Q. Morris, and J. Wrana. "Dynamic Modularity in Protein Interactions Networks Predicts Breast Cancer Outcome." *Nature Biotechnology*. 2009 1
- [11] S. Borgatti. "Centrality and Network Flow." *Social Networks*. (2005). 1
- [12] S. Borgatti and M. Everett. "A Graph-Theoretic Perspective on Centrality." *Social Networks*. (2006). 1
- [13] G. Ghoshal and A. Barabasi. "Ranking Stability and Super-Stable Nodes in Complex Networks." *Nature Communications*. 2011. 1
- [14] P. Brodka, P. Stawiak, and P. Kazienko. "Shortest Path Discovery in the Multilayered Social Network.? *International Conference on Advances in Social Networks Analysis*. 2011. 1
- [15] M. Domenico, A. Ribalta, E. Omodei, S. Gomez, and A. Arenas. "Ranking in Interconnected Multilayer Networks Reveals Versatile Nodes." *Nature Communications*. 2015. 1
- [16] P. Mucha, T. Richardson, K. Macon, M. Porter, and J.P. Onnela. "Community Structure in Time- Dependent, Multiscale, and Multiplex Networks." *Science*. 2010. 1
- [17] M. Domenico, C. Granell, M. Porter, A. Arenas. "The Physics of Spreading Processes in Multilayer Networks," *Nature Physics*. 2016. 1
- [18] L. Kwong, T. Heffernan, L. Chin. "A systems biology approach to personalizing therapeutic combinations." *Cancer Discovery*. 2013. 1

- [19] J. Utikal, J. Polo, M. Stadtfeld, N. Maherali, W. Kulalert, R. Walsh, A. Khalil, J. Rheinwald, and K. Hochedlinger. "Immortalization eliminates a road-block during cellular reprogramming into iPS cells." *Nature*. 2009. 1
- [20] E. Nicola. "When Bode meets Shannon: Control-oriented feedback communication schemes." *IEEE transactions on Automatic Control*. 2004. 1
- [21] S. R. S. Varadhan. "Large Deviations and Applications." *SIAM*. 1984. 1, 4
- [22] Y. Ollivier. "Ricci Curvature of Markov Chains on Metric spaces." *Journal of Functional Analysis*. 2009. 1, 4
- [23] Y. Ollivier. "Ricci Curvature of Metric Spaces." *C. R. Math. Acad. Sci. Paris*. 2007. 1
- [24] R. Sandhu, T. Georgiou, E. Reznik, L. Zhu, I. Kolesov, Y. Senbabaoglu, and A. Tannenbaum. "Graph Curvature for Differentiating Cancer Networks." *Nature (Scientific Reports)*. 2015. 1, 2, 3, 6
- [25] R. Sandhu, T. Georgiou, and A. Tannenbaum. "Ricci Curvature: An Economic Indicator for Market Fragility and Systemic Risk." *Science (Science Advances)*. 2016. 1, 2, 3
- [26] B. Anderson, D. Quist, J. Neil, C. Storlie, and T. Laine. "Graph-Based Malware Detection Using Dynamic Analysis." *Journal in Computer Virology*. 2011. 1
- [27] C. Wang, E. Jonckheere, and R. Banirazi. "Wireless network capacity versus Ollivier-Ricci curvature under Heat Diffusion (HD) protocol." *IEEE American Control Conference*. 2014. 1
- [28] P. Ranjan and E.H. Abed. "Nonlinear dynamics of TCP with RED control." *Workshop on Large-Scale Communication Networks: Topology, Routing, Traffic, and Control. Institute for Pure and Applied Mathematics (IPAM)*. 2002. 1
- [29] R. Sandhu, S. Lamhamedi-Cherradi, S. Tannenbaum, J. Ludwig, and A. Tannenbaum. "An Analytical Approach for Insulin-like Growth Factor Receptor 1 and Mammalian Target of Rapamycin Blockades in Ewing Sarcoma," *arXiv*. 2016. 1
- [30] S. Wagner and N. Neshat. "Assessing the Vulnerability of Supply Chains Using Graph Theory." *International Journal of Production Economics*. 2010. 1
- [31] A. Haldane and R. May. "Systemic risk in banking ecosystems." *Nature* 2011. 2
- [32] S. Battiston, G. Caldarelli, C. Georg, R. May, and J. Stiglitz. "Complex derivatives." *Nature Physics*. 2013. 2
- [33] C. Villani. *Optimal Transport, Old and New*. Springer-Verlag. 2008. 2, 3
- [34] T. Georgiou. "An Instrinsic metric for Power Spectral Density Functions." *IEEE Signal Processing Letters*. 2007. 2
- [35] S. Gustafson and I. M. Sigal. *Mathematical Concepts of Quantum Mechanics*. Springer. 2011. 2
- [36] Z. Chebb and M. Moahker. "Means of Hermitian positive-definite matrices based on the log-determinant alpha-divergence function." *Linear Algebra and Applications*. 2012. 2
- [37] F. Hai and D. Petz. "Riemannian geometry on positive definite matrices related to means." *Linear Algebra and Applications*. 2009. 2
- [38] S. Bonnabel and R. Sepulchre. "Geometric distance and mean for positive semi-definite matrices of fixed rank." *SIAM Journal of Matrix Analysis and Applications*. 2009. 2
- [39] H. Karcher. "Riemannian center of mass and mollifier smoothing." *Communications on Pure and Applied Mathematics*. 1977. 2
- [40] P. Jupp and K. Mardia. "A unified view of the theory of directional statistics." *International Statistical Review*. 1989. 2
- [41] M. Moakher. "Means and averaging in the group of rotations." *SIAM Journal of Matrix Analysis and Applications*. 2002. 2
- [42] A. Edelman, T. Arias, and S. Smith. "The Geometry of Algorithms with Orthogonality Constraints." *SIAM Journal of Matrix Analysis and Applications*. 2002. 2
- [43] L. Billera, S. Holmes, K. Vogtmann. "Geometry of the space of phylogenetic trees." *Advances in Applied Mathematics*. 2001. 2
- [44] C. Whidden and F. Matsen. "Ricci-Ollivier curvature of the rooted phylogenetic subtree-prune-regraft graph." *Theoretical Computer Science*. 2017. 2
- [45] S. Zairis, H. Khiabani, A. Blumberg, R. Rabadan. "Moduli spaces of phylogenetic trees describing tumor evolutionary patterns." *Lectures Notes in Computer Science*. 2014. 2
- [46] N. Taleb. "The Black Swan: The Impact of the Highly Improbable." *Random House*. 2007. 2
- [47] S. Haker, L. Zhu, and A. Tannenbaum. "Optimal Mass Transport for Registration and Warping," *International Journal of Computer Vision*. 2004. 3
- [48] J. Benamou and Y. Brenier. "A Computational Fluid Mechanics Solution to the Monge-Kantrovich Mass Transfer Problem." *Numerische Mathematik*. 2000. 3

- [49] W. Li, S. Osher, and W. Gangbo. "A Fast Algorithm for Earth Mover's Distance based on Optimal Transport and L1 Type Regularization." *arXiv*. 2016. 3
- [50] Y. Chen, T. Georgiou, and A. Tannenbaum. "Matrix Optimal Mass Transport: A Quantum Mechanical Approach." *arXiv*. 2016. 3, 4
- [51] R. Jordan, D. Kinderlehrer, and F. Otto. "The Variational Formulation of the Fokker-Planck Equation." *SIAM Journal on Mathematical Analysis*. 1998. 3
- [52] J. Lott and C. Villani. "Ricci Curvature for Metric-Measure Spaces via Optimal Transport." *Annals of Mathematics*. 2009.
- [53] K. Sturm. "On the geometry of metric measure spaces." *Acta Math*. 2006. 3
- [54] B. Chow, P. Lu, L. Ni. "Hamilton's Ricci Flow." *American Mathematical Society*. 2006. 3
- [55] Y. Rubner, C. Tomasi, and L. Guibas. "The Earth Mover's Distance as a Metric for Image Retrieval." *International Journal on Computer Vision*. 2000. 4
- [56] M. DoCarmo. *Riemannian Geometry*. Birkhauser. 1992. 4
- [57] K. Nomizu. "Invariant affine connections on homogeneous spaces." *American Journal of Math*. 1954. 4
- [58] P. Fletcher and S. Joshi. "Principal geodesic analysis on symmetric spaces: Statistics of diffusion tensors." *ECCV*. 2004 4
- [59] X. Pennec, P. Fillard, and N. Ayache. "A Riemannian Framework for Tensor Computing." *IJCV*. 2005. 4, 5, 7
- [60] V. Arsigny, P. Fillard, X. Pennec, and N. Ayache. "Log-Euclidean metrics for fast and simple calculus on diffusion tensors." *Magnetic Resonance in Medicine*. 2006. 4
- [61] Y. Rathi, A. Tannenbaum, O. Michailovich. "Segmenting Images on the Tensor Manifold." *CVPR*. 2007 4, 8
- [62] S. Helgason. *Differential Geometry, Lie Groups, and Symmetric Spaces*. Academic Press. 1978 4
- [63] S. Kobayashi and K. Nomizu. *Foundations of Differential Geometry*. Interscience Tracts in Pure and Applied Mathematics. 1969 4
- [64] F. Bauer, J. Jost, and S. Liu. "Ollivier-Ricci Curvature and the Spectrum of the Normalized Graph Laplace Operator." *arXiv*. 2013. 6
- [65] G Keller. "Embryonic stem cell differentiation: emergence of a new era in biology and medicine." *Genes Dev* 19, 1129-1155 2005. 7
- [66] C. Banerji, D. Saavedra, S. Severini, M. Widshwendter, T. Enver, J. Zhou, and A. Teschendorff. "Cellular network entropy as the energy potential in Waddington differentiation landscape." *Nature (Scientific Reports)*. 2013. 7